Local Site Effects Study On Ground Acceleration During The 1994 Northridge Earthquake
(1994年北嶺地震局部場址效應之研究)

Byau-Heng Chin
(秦葆珩)

Institute of Geophysics, National Central University
(國立中央大學地球物理研究所)

Abstract

The goal of this study is to investigate the local site response during the 1994 Northridge earthquake. First, the strong motion prediction method was validated by simulating 27 rock site stations. The agreement between the observed and predicted records was good for peak acceleration and response spectra. One-dimensional nonlinear site response analysis has been also used to reflect the representative soil condition. Then, the site amplification factor was calculated by comparing the observed motion at the surface soil sites with the predicted basement motion. A surface versus basement PGA curves derived from a site located in downtown Los Angeles also has been developed using 1-D nonlinear analysis. The data points are spread between the predicted curves for the linear and non-linear models. In general, the amplification is considerably greater at the lower ground motion than the corresponding amplification at the large ground motions.

1. Introduction

In this study, the site amplification factor was calculated by comparing the observed motion at the surface soil sites with the motion at the basement predicted for the given earthquake source and propagation path to the recording site.

The Loma Prieta earthquake data supported a universal relation between the surface peak ground acceleration (PGA) and the basement PGA applicable to all soil sites. On this basis, Aki and Chin (1994) tested a method for correcting the weak motion amplification factor for non-linearity based on the assumption that such a universal relation exists. This method was applied to the 1989 Loma Prieta and the 1992 Landers earthquake with encouraging results (Chin and Aki, 1993). In this study, however, from the Northridge earthquake data that the same universal relation does not apply to most soil sites. The relation between the observed surface PGA and the predicted basement PGA for the Northridge earthquake was found to be more complicated and show greater scatter than the case of the Loma Prieta earthquake. In order to develop better "universal" relation for the Los Angeles region, a new relation between the surface PGA and the basement PGA was developed at downtown Los Angeles site: Temple and Hope TAH (CDMG#24611) using 1-D nonlinear analysis.

2. Ground Motion Simulation For Rock Site Stations

A stochastic source model called "ω-squared model" proposed by Hanks and McGuire (1981) has gained broad support from the seismological community as a means to predict the amplitude spectra or peak values of strong ground motion for practical engineering application. In this study, the earthquake accelerations are considered to be band-limited random noise in the frequency band between the corner frequency fo and the high-cut frequency fmax. The corner frequency fo is related to the seismic moment Mo and stress parameters $\Delta\sigma$ by the Brune formula (1970, 1971). The observed spectra of strong ground motions usually show a rapid decrease with increasing frequency beyond a certain frequency fmax. The source model of ground motion prediction is based on the specific barrier of Papageorgiou and Aki (1983), in which the sub-event circular crack is replaced by the ω-squared model. The propagation path effect was approximated by the 1/R law of geometrical spreading in the range of 10 to 100 km and an attenuation factor Q(f).

The M=6.7 Northridge earthquake was recorded by many accelerographs operated by the California Division of Mines and Geology (CDMG) (Darragh et al., 1994), the United States Geological Survey (USGS) (Porcella et al., 1994) and the University of Southern California (Trifunac et al., 1994). Total 27 rock site and 93 soil site stations were used for this study as shown in Figure 1. The total fault plane was divided into 2 subevents separated by 10 km with equal seismic moment 0.6×10^{26} dyne-cm. The rupture is initiated at the southern sub-event and propagates northward with the rupture velocity of 2.4 km/sec. For each sub-event, the acceleration amplitude spectrum is represented as ω-squared model with the local stress drop $\Delta\sigma$= 150 bars and fmax =10 Hz. For the propagation path effect, we used the geometrical spreading 1/R and attenuation factor Q(f)=61f obtained by Papageorgiou and Aki (1983) from the 1971 San Fernando strong motion data.

The predicted peak acceleration and the observed values at each rock site station along with hypocentral distances are shown in Figure 2. The predicted value is designated by a solid triangle, the observed values are marked by open circles. The shaded area indicates a 84% confidence interval for the predicted PGA values and the solid curve represents the least-square fit through the attenuation relation of $\ln PGA = A_0 - \ln D + A_1$, where D is the hypocentral distance in km. Figure 3 shows the peak acceleration ratio of observed to the predicted as a function of predicted PGA. Dotted lines represent a 84% confidence interval. The predicted peak acceleration shows in good agreement with the observed for the whole distance range. We recognized that there still remains skepticism about the use of peak acceleration as a scaling parameter because the peak acceleration is a quantity that reflects different frequency bands at different. In this study, we also examine our prediction in terms of the spectral measurement of ground motion.

Quantitative comparisons were made for 5% damped response spectral values. Figure 4 shows the model bias of the observed response spectra relative to the calculated for 7 rock sites. Negative model bias corresponds to over-prediction of calculated response. Dotted lines represent a 90% confidence interval. The computed model bias is essentially zero at the 90% confidence interval for frequency between 0.1 to 10 Hz. The standard error is about 1.0 (in natural logarithm) for frequency at 10 Hz. A good agreement is found at all rock sites station to confirm the validation of modeling approach for the Northridge earthquake.

3. 1-D Nonlinear Site Response analysis at Downtown Los Angeles Site TAH

In order to provide a library of simulated time histories to augment the empirical data set of time histories recorded close to large earthquake, suites of rock time histories are generated for five scenario earthquakes in Southern California using a suite of state-of-the-art numerical simulation methods. Three time histories were selected for each scenario event at site Temple and Hope (TAH) in the downtown LA region. The selection considered the spectral content, comparison to empirical attenuation, and applicability of the model to the specified magnitude and distance. The three time histories (single horizontal component) should represent a realistic range of the characteristic of the ground motion for both magnitude and waveform. One-dimensional nonlinear site response analysis has been used to modify these selected time histories to reflect representative soil condition. A non-linear explicit finite difference program DETRAN (Lam et al., 1978) which is a modified version of the program NONLI3 (Joyner and Chen, 1975) has been used to calculate the 1-D nonlinear site response.

For 1D soil response analysis, a constitutive relationship that relates stress and strain is required. It is composed of an initial loading curve and of hysteresis loops developed upon unloading-reloading. The program DETRAN models the hysteretic behavior of the soil by the composite elastic-plastic sub-elements (Iwan, 1967). In this study, the modulus reduction curves as a function of strain amplitude were used to derive the non-linear shear stress-strain backbone curve necessary to determine the elastic-plastic subelements of Iwan model. The hysteristic behavior inherent in the Iwan model leads to damping behavior reasonably similar to that at the damping curves shown.

The site amplification factors were calculated as the ratio of 5% damping response spectral acceleration computed at the surface of site TAH for each scenario earthquakes to 5% damping response spectral acceleration of basement motion. Response spectral values are usually assumed to log-normally distributed, therefore, we take the natural logarithm of the spectral acceleration on each input basement motion (INP) and calculated surface motion

(CAL). Figure 5 shows the averaged amplification factors calculated from three time-history pairs for five scenario earthquakes. The peak ground acceleration for input basement motion of the three time histories for five scenarios are also shown inside the parenthesis. At lower levels of shaking (i.e. the earthquake scenarios PV1, PV2 and SA1), the amplification factors show a similar trend on average, having its greatest amplification effects near the fundamental resonance of the median profile at a frequency of about 1-2 Hz. Above frequencies of about 2 Hz, the amplification factors begin to saturate to a factor of about 1.6. For the higher input motions (i.e. the earthquake scenarios EP1 and EP2), the computed amplification factors show a sharp decrease with increase in frequency and are less than one above 3 Hz. The minimum amplification factor value is about 0.6. At lower frequencies (less than 1 Hz), there are some reversals to this trend. This may associated with a shifting and an accompanying increase in amplitude of resonance along with an increase in amplification due to a greater velocity gradient for higher levels of input motion.

4. Relationship Between Observed Alluvial Site PGA Versus Predicted Basement Site PGA

The basement motion PGA for each soil site station was calculated by using a model of homogeneous half-space. The observed PGA at soil site stations as a function of predicted basement motion PGA are shown in Figure 6a. Figure 6b shows the ratio of the observed PGA to the predicted basement motion PGA as a function of predicted basement motion PGA. The calculated peak acceleration at the surface as a function of the peak acceleration of the basement motion using three input time histories are represented as smooth curves shown in Figure 6a and Figure 6b. For comparison, the result using a linear model is also shown by dotted lines.

For the basement PGA greater than 0.2 g, station ST60 (USC#55) tend to agree with the prediction for the linear model. The stations ST62 (USC#57), ST61 (USC#56), ST40 (USC#13), and ST28 (Jensen Filter Plant) show agreement with the nonlinear model. In this study, the data points are spread between the predicted curves for the linear and non-linear models for the soil response at the site TAH. The stations ST1 (Arleta), ST36 (USC#3), ST37 (USC#53), ST38 (USC#9), ST58 (USC#53), and ST63 (USC#58) fall below the nonlinear curves, on the other hand, the stations ST2 (Sylmar) and ST27 (Sepulveda VA hospital) fall above the nonlinear curves. At lower basement accelerations, the stations such as ST7 (Santa Monica), ST10 (LA Obregon Park) are clearly close to the linear model. At basement PGA less than 0.1 g, all the observations agree with calculated results for the linear model.

Sugito and Kameda (1990) developed a method for calculating amplification factor between soil and rock surface strong motion including non-linear amplification effect of soil layers overlying bedrocks. They defined the conversion factor β_a as the ratio of peak acceleration at soil surface to that at the rock surface, and estimate β_a for typical soil conditions specified by geotechnical parameters S_n and d_p. Their result is shown in the lower left corner of the figure 7, where the flat part of β_a value corresponds to the linear response region and decrease from flat level indicates the degree of non-linearity. The amount of decrease depends on the soil parameters (S_n , d_p) and acceleration at the rock surface A_r. The parameters d_p gives the depth to the bed rock where the shear wave velocity is approximately 600~700 m/sec, and the parameter S_n is calculated from the blow-count (N-value) profile obtained from the standard penetration test. Our simulation results for the sediment sites are also shown in Figure 7, where we plot the ratio of the observed peak acceleration to the predicted basement motion as a function of predicted basement peak acceleration. As shown in Figure 7, our results are expected from that of Sugito and Kameda both in the magnitude of departure from the linear prediction and in the threshold acceleration level beyond which the non-linearity begin. For comparison, the results using 1-D linear and nonlinear model are also shown in the Figure.

5. Conclusion

The wealth of data from the 1994 Northridge earthquake have been examined by the same method as previously applied to the 1989 Loma Prieta earthquake and the 1992 Landers earthquake. Conclusions obtained from them are also similar to those obtained from the Loma Prieta earthquake data.

The relation between the observed surface PGA and the predicted basement PGA for the

Northridge earthquake was found to be more complicated and show greater scatter than in the case of the Loma Prieta earthquake. We found from the Northridge earthquake data that the amplification is considerably greater at the lower ground motion than the corresponding amplification at the large ground motions

For this purpose, an amplification factor as a function of input rock motion curve was derived from a downtown Los Angeles site TAH using the 1-D nonlinear analysis. The magnitude of departure from the linearity and the threshold acceleration level beyond which the non-linearity is detected in our study appear to be well within the range expected by geotechnical engineers.

6. References

Aki, K. and Chin, B.H.. The use of coda waves for characterizing the site effect on strong ground motion, *Proc. Structure Congress XII, ASCE,* Vol. 1,579-584, (1994).

Brune, J. N.. Tectonic stress and the spectra of seismic shear waves from earthquakes, *J. Geophys. Res.*, 75, 4997-5009, (1970).

Brune, J. N.. Correction *J. Geophys. Res.*, 76, 5002, (1971).

Chin, B.H. And Aki, K.. Strong motion simulation during the 1992 Landers earthquake, *EOS-Trans. AGU*, Vol. 74, No. 43, 421, (1993).

Darragh, R., Cao, T., Cramer, C., Graizer, V., Huang, M. and Shakal, A.. Processed CSMIP strong-motion records from the Northridge, California earthquake of January 17 1994: release No. 4, *Calif. Div. Mines and Geology, Office of Strong Motion Studies, Report No. OSMS* 94-10, (1994).

Hanks, T. C. and McGuire, R.K.. The character of high-frequency strong ground motion, *Bull. Seism. Soc. Am.* 71, 2071-2095, (1981).

Iwan, W.D. (1967). On a class of models for the yielding behavior of continuous and composite system, *J. of Applied Mechanics* 34, 612-617.

Joyner, W.B. and Chen, A.F.T.. Calculation of nonlinear ground response in earthquakes, *Bull. Seism. Soc. Am.* 65, 1315-1336, (1975).

Lam, I., Tsai, C.F. and Martin, G.F.. Determination of site dependent spectra using nonlinear analysis, *2_nd Inter. Conf. on Microzonation,* San Franciaco, California, 1089-1194, (1978).

Papageorgiou, A.S. and Aki, K.. A specific barrier model for the quantitative description of inhomogeneous faulting and the prediction of strong ground motion, Part I: description of the model, *Bull. Seism. Soc. Am.* 73, 693-722, (1983).

Porcella, R.L., Etheredge, E.C., Maley, R.P., and Acosta, A.V.. Accelerograms recorded at USGS national strong-motion network during the Ms=6.6 Northridge, California earthquake of January 17, 1994, *U.S. Geol. Surv., Open-file Rept. 94-141*, 100p, (1994).

Sugito, M. and H. Kameda (1990). Nonlinear soil amplification factor model with verification by vertical strong motion array records, *4th U.S. National Conf. Earthquake Engineering,* 1-10.

Trifunac, M.D, Todorovska, M.I. and Ivanovic, S.S.. A note on distribution of uncorrected peak ground accelerations during the Northridge, California, earthquake of 17 January 1994, *Soil Dyn. and Earthq. Engrg.*, 13, 187-196, (1994).

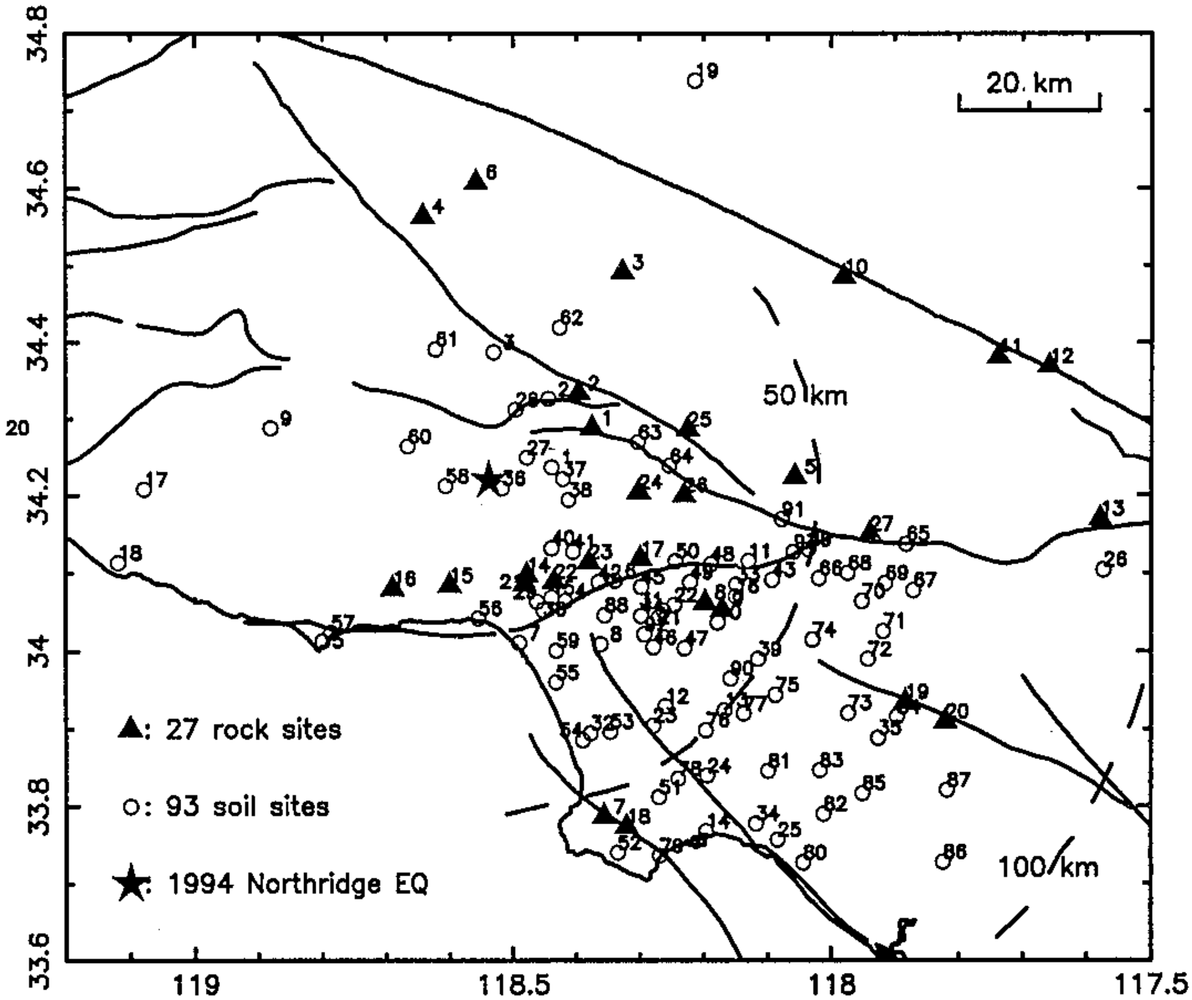

Figure 1. Locations of stations used in this study.

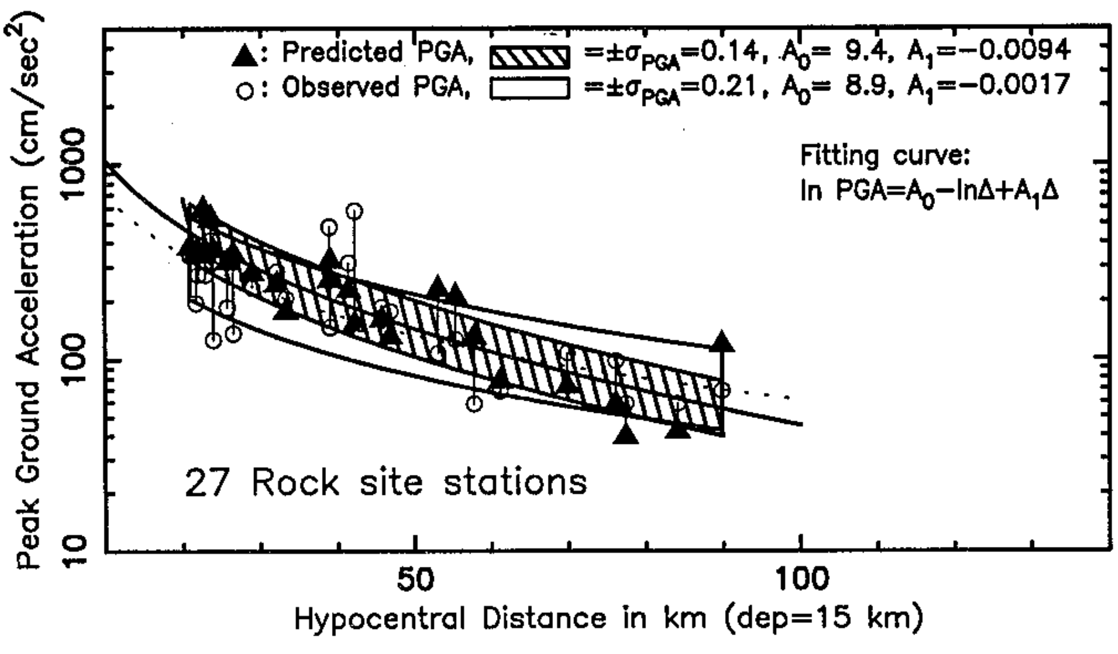

Figure 2. The predicted peak acceleration and the observed values at 27 rock site stations along with hypocentral distances.

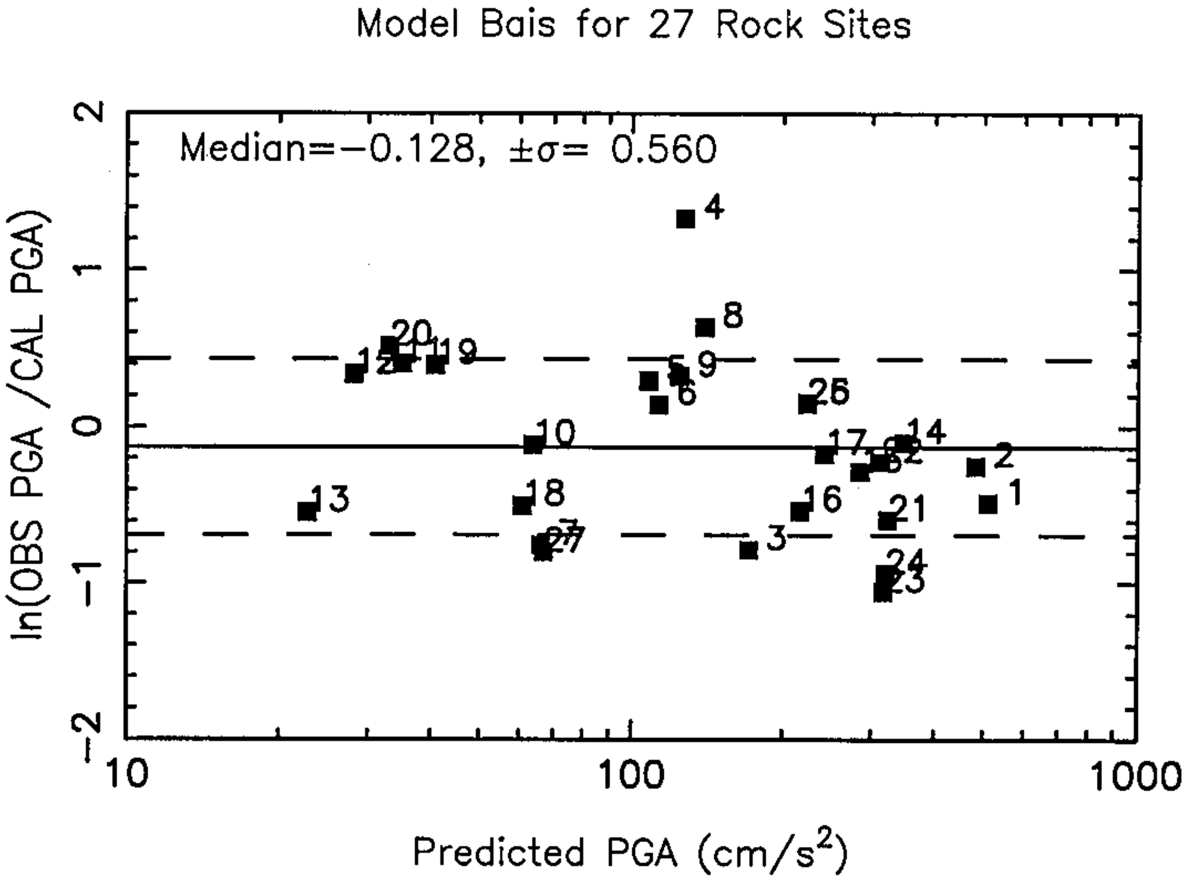

Figure 3. The mean residual (model bias) of PGA for 27 rock sites stations. The dotted lines show the 84% confidence interval.

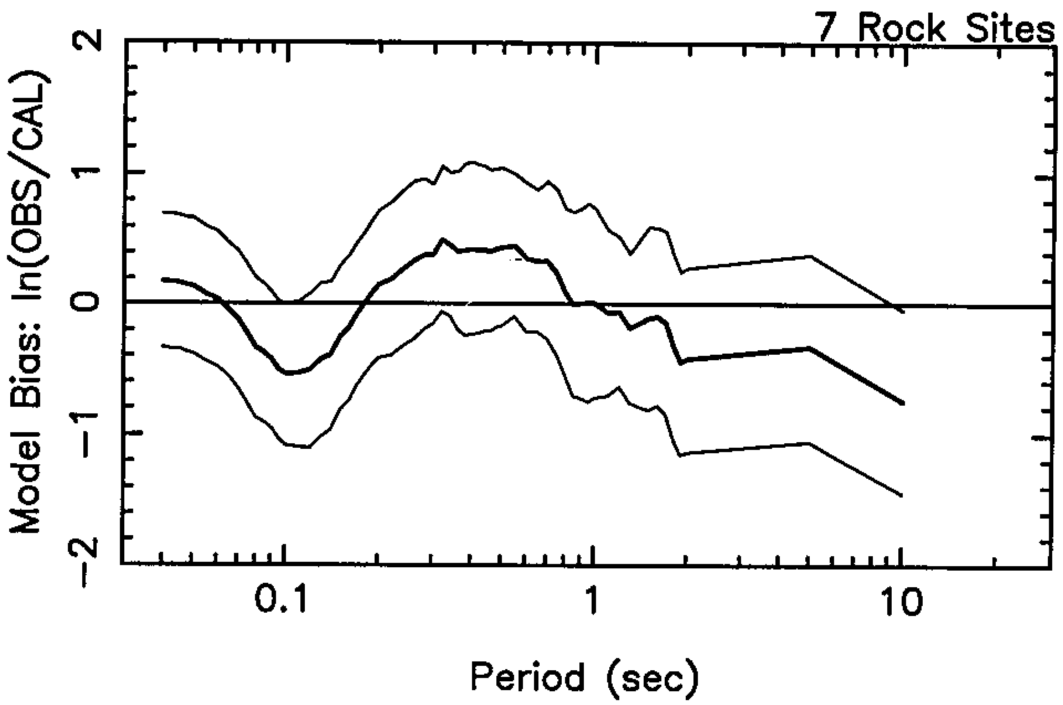

Figure 4. The model bias of observed relative to calculated 5% damped response spectra for the 7 rock site stations. The dotted lines show the 90% confidence interval.

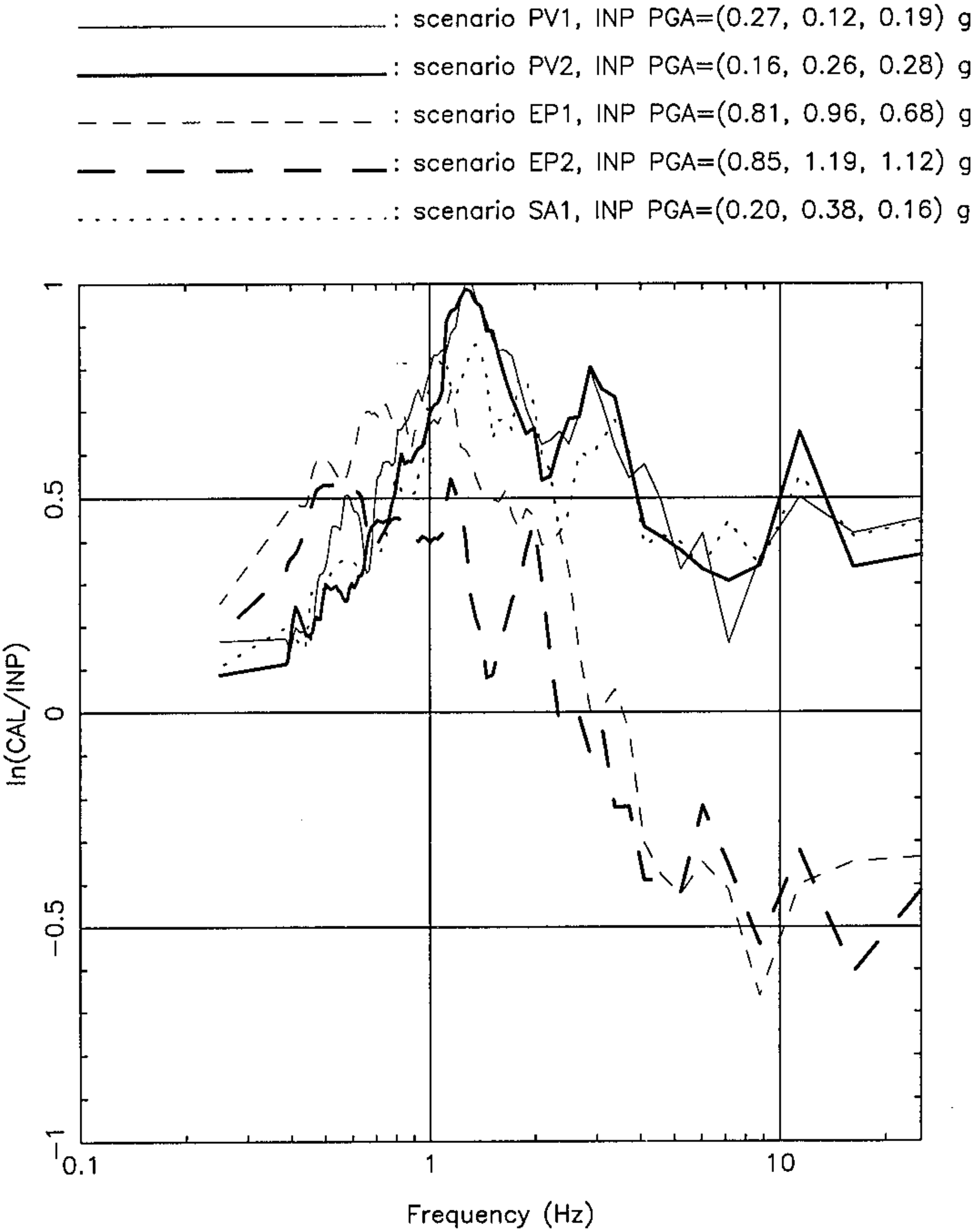

Figure 5. The averaged amplification factor calculated from three time-history pairs for five scenario earthquakes.

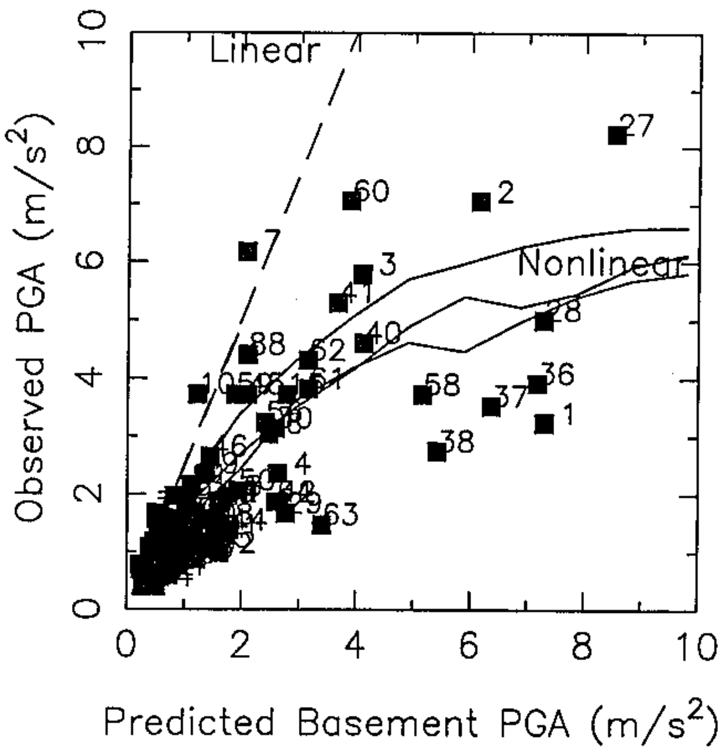

Figure 6a. The observed alluvial site PGA versus predicted basement motion PGA during the 1994 Northridge earthquake.

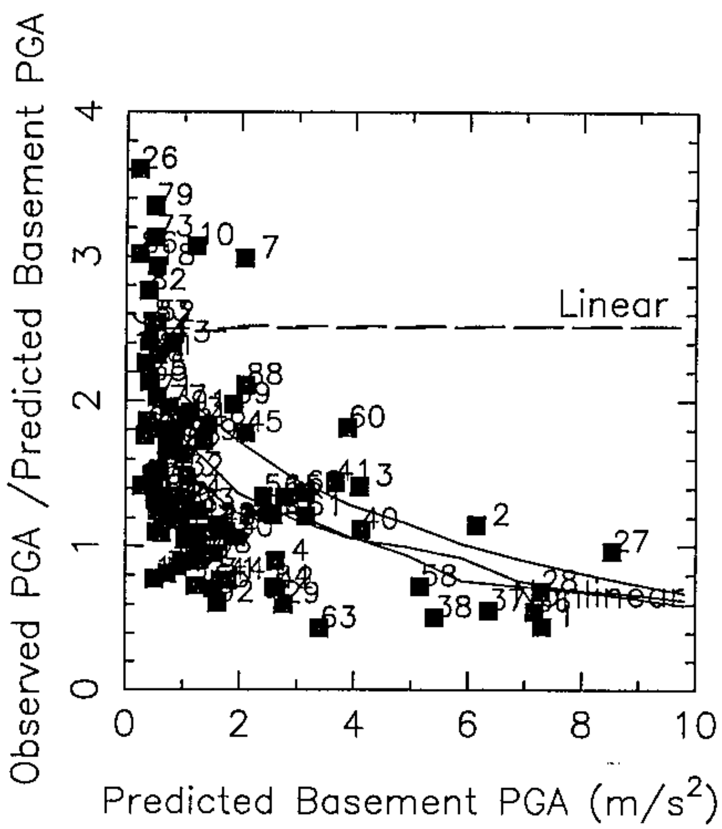

Figure 6b. The ratio of observed alluvial site PGA to predicted basement motion PGA as a function of predicted basement motion PGA.

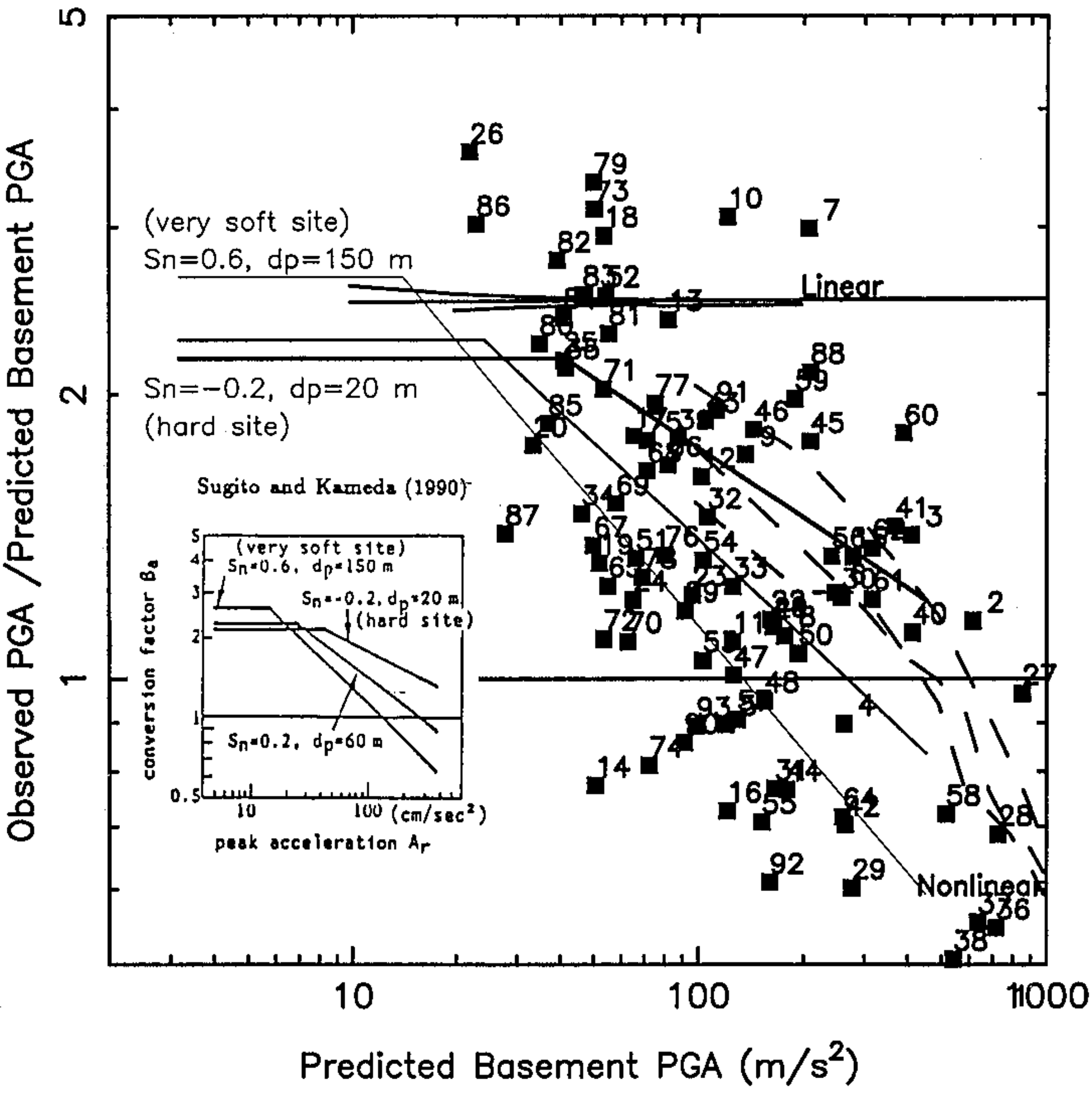

Figure 7. The inset figure in the lower left corner shows the conversion factor as a function of bedrock acceleration calculated by Sugito and Kameda (1990). The large figure shows the ratio of observed peak acceleration to predicted basement motion as a function of predicted basement motion PGA. This figure is directly comparable to the inset figure.